Synthesis, Cytotoxicity Evaluation and Molecular Docking Studies of Xanthyl-Cinnamate Derivatives as Potential Anticancer Agents

Muthia Rahayu Iresha[1,2], Jumina Jumina[1*], Harno Dwi Pranowo[1,2], Eti Nurwening Sholikhah[3], and Faris Hermawan[1,2]

[1]*Department of Chemistry, Faculty of Mathematics and Natural Sciences, Universitas Gadjah Mada, Sekip Utara, Yogyakarta 55281, Indonesia*

[2]*Austrian-Indonesian Centre (AIC) for Computational Chemistry, Department of Chemistry, Faculty of Mathematics and Natural Sciences, Universitas Gadjah Mada, Sekip Utara, Yogyakarta 55281, Indonesia*

[3]*Department of Pharmacology and Therapeutics, Faculty of Medicine, Public Health and Nursing, Universitas Gadjah Mada, Sekip Utara, Yogyakarta 55281, Indonesia*

** **Corresponding author:***

email: jumina@ugm.ac.id

Received: July 11, 2022
Accepted: September 3, 2022

DOI: 10.22146/ijc.76164

Abstract: *A new series of xanthyl-cinnamate hybrid compounds (**4a-d**) have been synthesized and screened through* in vitro *assay against four human cancer cell lines, i.e., HeLa, T47D, A549, and WiDr. The results revealed that xanthone hybridization with cinnamic acid increases the selectivity of the compounds with SI values of 2.75–209.03 compared to its parent oxygenated-xanthone. Compound 1,3-dihydroxyxanthen-6-yl cinnamate (**4c**) showed high cytotoxic activity against WiDr cell lines with an IC_{50} value of 39.57 μM. Molecular docking studies revealed the possible binding modes of all hybrid compounds with EGFR protein. A complex of 3,6-dihydroxyxanthen-1-yl cinnamate (**4d**)-EGFR, as the best binding model, exhibited higher predicted EGFR inhibitory activity than erlotinib and oxygenated-xanthone with a ΔG and Ki value of -35.02 kJ/mol and 0.74 μM, respectively. Compounds **4c** and **4d** were chosen as the most potent derivates from the study.*

Keywords: *xanthyl-cinnamate; xanthone; cinnamic acid; anticancer; hybrid molecule*

■ INTRODUCTION

The serious challenges in cancer treatment are still ongoing nowadays as cancer recorded a high mortality rate and rapidly increased incidence every year in all countries [1]. Chemotherapy, along with surgery and radiation therapy, is one of the three standard cancer treatments; however, some available medicines show low effectiveness and significant adverse effects on the human body [2]. Thus, they lead to the necessity of developing a new anticancer that will give better activity and overcome the high toxicity of current drugs.

Extensive research on the xanthone derivatives as anticancer agents has been published, revealing improved *in vitro* activity and drug-like characteristics [3-5]. Xanthone is an oxygenated heterocyclic aromatic molecule with a central pyran ring. Because of its structure rigidity [6], xanthone serves as a privileged structure in biological profiling. It was thoroughly reported that introducing additional substituents to the xanthone skeleton enhances its anticancer activity significantly. For instance, Fatmasari et al. [7] reported the synthesis of oxygenated xanthones as the anticancer agent against HeLa, WiDr, and MCF-7; however, these compounds were found to be toxic to normal cells. On the other hand, Yuanita et al. [8] have synthesized new xanthone derivatives through the attachment of halogen groups into oxygenated xanthones. The *in vitro* cytotoxicity study of chloroxanthone compounds against P388, HepG2, T47D, and HeLa cell lines revealed that the chloro-group enhanced the oxygenated xanthone anticancer activity, as well as decreased their toxicity properties.

Modification in the oxygenated xanthones structure through a molecular hybridization technique has also been investigated to discover and widen the potential application of these compounds as anticancer drugs. Cinnamic acid has been reported as an attractive anticancer candidate [9] due to its ability to induce apoptosis which causes cell death. This compound also causes cytoskeleton disruption in human melanoma cells [10]. Keawsa-ard et al. [11] reported the isolation of trans-cinnamic acid from *Solanum spiral* Roxb. leaves and its evaluation as the anticancer agent against oral KB, MCF-7, and NCI-H187 cancer cell lines. It was found that trans-cinnamic acid compounds have non-toxic properties in contrast to the used positive control Ellipticine. This cinnamoyl moiety was also observed in various types of biologically active substances and has been used to build new active compounds for anticancer [12-13], antiproliferative [14], anti-inflammatory [15] and antimicrobial [16] agents. Through maintaining the cinnamate structure, the molecular hybridization approach can be used by combining this compound with other active compounds to design a more active anticancer agent [17]. In the drug discovery field, the development of hybrid molecules by combining distinct pharmacophores may result in new compounds with outstanding biological characteristics. Furthermore, this technique may yield molecules with altered selectivity profiles, multiple modes of action, and decreased toxicities [18].

Based on the above findings, molecular hybridization of xanthone with cinnamate moiety was conducted in this study to obtain new efficient anticancer compounds with higher selectivity. All hybrid compounds were evaluated for their *in vitro* cytotoxicity activities against Hela, T47D, A549, WiDr, and Vero cell lines. In addition, molecular docking studies of the xanthyl-cinnamates against EGFR protein were conducted to determine the predicted binding mode of the hybrid compounds as anticancer agents.

■ EXPERIMENTAL SECTION

Materials

All chemicals and solvents used in the synthesis were from commercial sources without any further purification. Phloroglucinol (**2a**), resorcinol (**2b**), potassium carbonate (K_2CO_3), acetone, and acetonitrile were purchased from Merck. Eaton's reagent, salicylic acid (**1a**), and 2,4-dihydroxybenzoic acid (**1b**) were purchased from Sigma-Aldrich. The cell lines used for the cytotoxicity evaluation were human cervix carcinoma (HeLa, ATCC CCL-2), human breast cancer (T47D, ATCC HTB-133), colon adenocarcinoma (WiDr, ATCC CCL-218), adenocarcinoma human alveolar basal epithelial (A549, ATCC CCL-185), and kidney of an African green monkey (Vero, ATCC CCL-81). The materials used for the cytotoxicity evaluation were Dulbecco's Modified Eagle Medium (DMEM), media 199 (M199), Fetal Bovine Serum (FBS), penicillin-streptomycin (Pen-Strep), mycoxpert mycoplasma, fungizone, trypsin-EDTA solution, dimethyl sulfoxide (DMSO), phosphate-buffered saline (PBS), 3-(4,5-dimethylthiazol-2-yl)-2,5-diphenyltetrazolium bromide (MTT), HCl 0.01 M, and sodium dodecyl sulfate (SDS). Parasitology Laboratory, Universitas Gadjah Mada, supplied all the cells and other materials needed in the experiment.

Instrumentation

The ^{1}H- and ^{13}C-NMR spectra were recorded using a JNM-ECZ500R/S1 and JNM-ECS400 (^{1}H 500 MHz and 400 MHz, and ^{13}C 125 MHz and 100 MHz), respectively, using DMSO-d_6 and CD_3OD as solvent. The chemical shifts were shown relative to tetramethylsilane (TMS) as an internal standard in the deuterated solvent. Two dimensional-NMR experiments were performed using Heteronuclear Multiple Bond Correlation (HMBC, JNM-ECZ500R/S1) and Heteronuclear Multiple Quantum Coherence (HMQC, JNM-ECZ500R/S1). The mass spectra were obtained from either a direct-ionization mass spectrometer (DI-MS, Shimadzu QP2010S) or an ultra-performance liquid chromatography (UPLC) unit (LC: ACQUITY UPLC® H-Class System, Waters, USA) coupled with a mass spectrometer (Xevo G2-S QTof, Waters, USA). The IR spectra were taken on a Fourier-transform infrared spectrometer (FTIR, Shimadzu-Prestige 21). Purifications of the compounds were performed on

thin-layer preparative chromatography using Merck silica gel 60 (GF_{254}) plates and flash chromatography using Merck silica gel 60 (0.040–0.063 mm).

Procedure

General procedure for the synthesis of hydroxyxanthones (3a-c)

Compounds **3a**-**c** were synthesized in 11.79–48.25% yield from the cyclization reaction of phenol derivatives (5 mmol) and benzoic acid derivatives (5 mmol) with the addition of Eaton's reagent (5 mL). The mixture was stirred at 80 °C for 3 h. The mixture was cooled to room temperature, poured onto crushed ice, and allowed to stand for 1 h. The resulting solid was collected by filtration, washed with water, and dried in a desiccator. The purifications were performed with two kinds of methods: column chromatography (gradually 0–40% ethyl acetate in *n*-hexane) and thin layer preparative chromatography (*n*-hexane/ethyl acetate 7:3). The structure of all products was confirmed using ^{1}H-NMR, ^{13}C-NMR, FTIR, and DI-MS.

1,3-Dihydroxyxanthone (3a). Yield: 48.25% (yellow solid); ^{1}H-NMR (CD_3OD, 500 MHz): δ (ppm) 6.17 (1H, CH_{Ar}, d, J = 2.3 Hz, H2), 6.32 (1H, CH_{Ar}, d, J = 2.3 Hz, H4), 7.38 (1H, CH_{Ar}, t, H7), 7.45 (1H, CH_{Ar}, d, J = 8.5 Hz, H5), 7.75 (1H, CH_{Ar}, t, H6), and 8.16 (1H, CH_{Ar}, d, J = 7.5 Hz, H8). ^{13}C-NMR (CD_3OD, 125 MHz): δ (ppm) 93.92 (CH_{Ar}, C4), 98.01 (CH_{Ar}, C2), 102.46 (C_{Ar}, C9a), 117.37 (CH_{Ar}, C5), 120.35 (C_{Ar}, C8a), 123.82 (CH_{Ar}, C7), 125.19 (CH_{Ar}, C8), 135.00 (CH_{Ar}, C6), 156.07 (C_{Ar}, C10a), 158.13 (C_{Ar}, C4a), 163.51 (C–OH, C3), 166.72 (C–OH, C1), and 180.39 (C=O, C9). IR (KBr) ν/cm^{-1}: 1157 (C–O), 1566 (C=C), 1613 (C=C), 1651 (C=O), and 3325 (O–H). DI-MS m/z = 228 $[M]^+$, 200, 171, 92, 77, 51, 39.

1-Hydroxyxanthone (3b). Yield: 11.79% (yellow solid); ^{1}H-NMR (CD_3OD, 500 MHz): δ (ppm) 6.77 (1H, CH_{Ar}, d, J = 7.6 Hz, H2), 6.99 (1H, CH_{Ar}, d, J = 7.8 Hz, H4), 7.44 (1H, CH_{Ar}, t, H7), 7.56 (1H, CH_{Ar}, d, J = 8.5 Hz, H5), 7.65 (1H, CH_{Ar}, t, H3), 7.83 (1H, CH_{Ar}, t, H6), and 8.24 (1H, CH_{Ar}, d, J = 8.0 Hz, H8). ^{13}C-NMR (CD_3OD, 125 MHz): δ (ppm) 108.05 (CH_{Ar}, C4), 109.73 (C_{Ar}, C9a), 111.16 (CH_{Ar}, C2), 118.95 (CH_{Ar}, C5), 121.53 (C_{Ar}, C8a), 125.30 (CH_{Ar}, C7), 126.62 (CH_{Ar}, C8), 137.06 (CH_{Ar}, C6), 138.16 (CH_{Ar}, C3), 157.52 (C_{Ar}, C10a), 157.65 (C_{Ar}, C4a), 162.92 (C–OH, C1), and 183.51 (C=O, C9). IR (KBr) ν/cm^{-1}: 1234 (C–O), 1474 (C=C), 1613 (C=C), 1651 (C=O), and 3449 (O–H). DI-MS m/z = 212 $[M]^+$, 184, 155, 92, 77, 51, 39.

1,3,6-Trihydroxyxanthone (3c). Yield: 15.39% (yellow solid); ^{1}H-NMR (CD_3OD, 400 MHz): δ (ppm) 6.12 (1H, CH_{Ar}, d, J = 2.0 Hz, H2), 6.25 (1H, CH_{Ar}, d, J = 2.0 Hz, H4), 6.71 (1H, CH_{Ar}, d, J = 2.4 Hz, H5), 6.80 (1H, CH_{Ar}, dd, J = 9.0 and 2.4 Hz, H7), and 7.95 (1H, CH_{Ar}, d, J = 9.0 Hz, H8). ^{13}C-NMR (CD_3OD, 100 MHz): δ (ppm) 93.65 (CH_{Ar}, C4), 97.68 (CH_{Ar}, C2), 101.77 (CH_{Ar}, C5), 102.06 (C_{Ar}, C9a), 112.93 (C_{Ar}, C8a), 113.41 (CH_{Ar}, C7), 126.96 (CH_{Ar}, C8), 158.07 (C_{Ar}, C10a), 158.12 (C_{Ar}, C4a), 163.34 (C–OH, C6), 164.39 (C–OH, C3), 165.37 (C–OH, C1), and 179.91 (C=O, C9). IR (KBr) ν/cm^{-1}: 1180 (C–O), 1458 (C=C), 1574 (C=C), 1613 (C=O), and 3503 (O–H). DI-MS m/z = 244 $[M]^+$, 215, 137, 187, 108, 93, 69, 51, 39.

General procedure for the synthesis of xanthyl-cinnamate (4a-d)

The syntheses were performed according to the previous method by replacing 1,3-dibromopentane with cinnamoyl chloride [19]. The synthesis of the xanthyl-cinnamate was performed by reacting hydroxyxanthone (0.2 mmol) with cinnamoyl chloride (0.2 mmol) in the

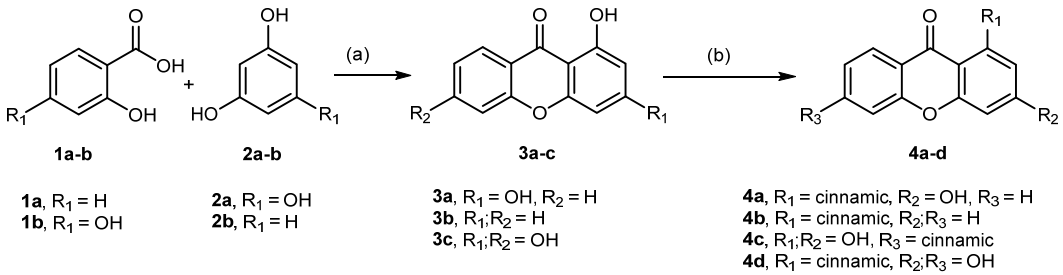

Scheme 1. Synthesis of hybrid compounds **4a**-**d**: (a) Eaton's reagent (5 mL), 80 ± 3 °C, 3 h; (b) K_2CO_3 (0.25 mmol), acetone/acetonitrile 1:2 (v/v), 70 ± 5 °C, 4–5 h

presence of K_2CO_3 (0.25 mmol) in acetone/acetonitrile media. The mixture was stirred at 70 °C for 4–5 h. The progress of the reaction was monitored using the TLC technique. Upon completion, the desired compound was filtered, and the solvent was evaporated. The solid product obtained was purified by thin layer preparative chromatography (*n*-hexane/ethyl acetate = 7:3). The structure of all compounds was confirmed using ^{1}H-NMR, ^{13}C-NMR, HMQC, HMBC, FTIR, DI-MS, and LC-MS.

3-Hydroxyxanthen-1-yl cinnamate (4a). Yield: 15.92% (yellow solid); ^{1}H-NMR (DMSO-d_6, 500 MHz) and ^{13}C-NMR (DMSO-d_6, 125 MHz) data, see Table 1. IR (KBr) ν/cm^{-1}: 1134 (C–O), 1466 (C=C), 1574 (C=C), 1628 (C=O), 1744 (C=O α,β-unsaturated ester), and 3449 (O–H). DI-MS *m/z* = 358 [M]$^+$, 267, 228, 199, 171, 131 (base peak), 103, 77, 51, 39.

Xanthen-1-yl cinnamate (4b). Yield: 10.09% (white crystal); ^{1}H-NMR (DMSO-d_6, 500 MHz) and ^{13}C-NMR (DMSO-d_6, 125 MHz) data, see Table 1. IR (KBr) ν/cm^{-1}: 1134 (C–O), 1474 (C=C), 1613 (C=C), 1667 (C=O), and 1721 (C=O α,β-unsaturated ester). LC-MS *m/z* = 343 [M+H]$^+$.

1,3-Dihydroxyxanthen-6-yl cinnamate (4c). Yield: 17.91% (yellow solid); ^{1}H-NMR (DMSO-d_6, 400 MHz) and ^{13}C-NMR (DMSO-d_6, 100 MHz) data, see Table 1. IR (KBr) ν/cm^{-1}: 1165 (C–O), 1451 (C=C), 1613 (C=C), 1651 (C=O), 1713 (C=O α,β-unsaturated ester), and 3426 (O–H). LC-MS *m/z* = 375 [M+H]$^+$.

3,6-Dihydroxyxanthen-1-yl cinnamate (4d). Yield: 12.70% (yellow solid); ^{1}H-NMR (DMSO-*d6*, 400 MHz) and ^{13}C-NMR (DMSO-d_6, 100 MHz) data, see Table 1. IR (KBr) ν/cm^{-1}: 1134 (C–O), 1458 (C=C), 1605 (C=C), 1628 (C=O), 1736 (C=O α,β-unsaturated ester), and 3426 (O–H). LC-MS *m/z* = 375 [M+H]$^+$.

Cytotoxicity evaluation

MTT assay was performed to evaluate the cytotoxicity activity of all synthesized compounds. Malignant and normal cell lines were cultured and dispensed into a 96-well plate; incubated at 37 °C in an incubator with 5% CO_2. Doxorubicin and cisplatin were chosen as positive controls. Four xanthyl-cinnamate derivates and three oxygenated-xanthones were screened at two-fold serial dilutions after diluting the corresponding solid in DMSO. After the cell exposure to the tested compounds for 24 h, the MTT solution was added to each well and placed in an incubator for 4 h. The plate was stored in a darkroom overnight after adding SDS solution. The absorbance was measured using an ELISA reader at a fixed wavelength of 595 nm. Each concentration of samples was assayed in triplicate, and the experiment was repeated biologically once or twice. The growth inhibition percentage of the cells is calculated and expressed in IC_{50}, which represents the effective concentration required to inhibit 50% of cell growth.

Molecular docking

The crystal structures of EGFR in the complex with erlotinib (PDB ID: 1M17) were obtained from the Protein Data Bank (www.rcsb.org). Erlotinib was used as an EGFR native ligand. The protein and native ligand were prepared by Chimera software and saved in .pdb format. The three-dimensional structure of all xanthone derivatives (**3a**-**c** and **4a**-**d**) was prepared and optimized in Gaussian 09 using DFT (B3LYP/3-21G) prior to the molecular docking studies. The molecular docking simulations were performed similarly to the previous study [20]. The grid box was defined using a 60 Å box (x, y, and z) with 0.375 Å of spacing. All parameters were kept as default. Afterward, the binding energy (ΔG) and inhibition constants (Ki) of xanthone derivatives and the native ligand that interacted with protein targets were calculated using AutoDock 4.2 software. These parameters were used by the program to score and rank each structure. Then, the molecular docking results were visualized using Discovery Studio Visualizer 2019.

■ RESULTS AND DISCUSSION

Synthesis of Xanthyl-Cinnamate

Compounds **3a**-**c** were successfully prepared by cyclization of phenol derivatives and benzoic acid derivatives using Eaton's reagent. The oxygenated xanthones were used as starting material for the further synthesis step. The xanthones were mixed with cinnamoyl chloride in the presence of potassium carbonate to produce the xanthyl-cinnamate derivatives. Acetonitrile was used as the solvent to produce

compounds **4a**-**b**, while acetone-acetonitrile (1:2) was utilized to produce compounds **4c**-**d** (Fig. 1). The synthesis route of xanthyl-cinnamate in this work is shown in Scheme 1. All the new compounds were characterized by ^{1}H-NMR, ^{13}C-NMR, MS, FTIR, HMQC, and HMBC. The spectral data of the synthesized compounds are given in Table 1. In general, the FTIR spectra of xanthyl-cinnamate showed the appearance of C=O ester groups at 1705–1745 cm^{-1}, indicating the characteristic of cinnamate moiety, while the C=O functional group of xanthone structure appeared at 1628–1667 cm^{-1}.

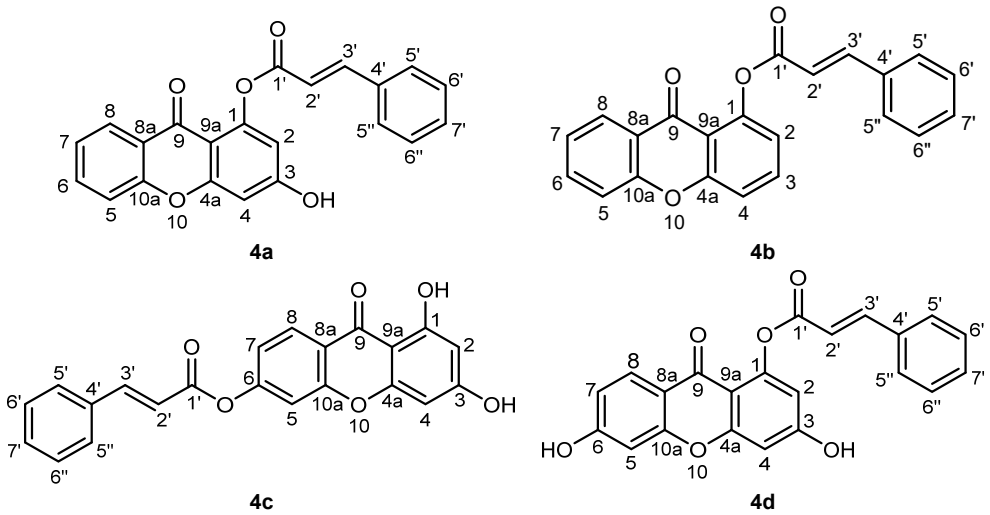

Fig 1. The structure of the synthesized xanthyl-cinnamate hybrid compounds

Table 1. ^{1}H-, ^{13}C-NMR, and HMBC spectra data for compounds 3-hydroxyxanthen-1-yl cinnamate (**4a**) and xanthen-1-yl cinnamate (**4b**)

Position	**4a**			**4b**		
	δ_H (*J* in Hz)	δ_C, type	HMBC	δ_H (*J* in Hz)	δ_C, type	HMBC
1	-	156.94, CO	-	-	157.19, CO	
2	7.05, d (2.1)	102.00, CH_{Ar}	C1, C9a	7.63, d (8.4)	116.96, CH_{Ar}	C1, C9a
3	-	162.57, C–OH	-	7.87, t	136.24, CH_{Ar}	C4a
4	6.76, d (2.1)	105.17, CH_{Ar}	C2, C3, C4a, C9a	7.21, d (7.9)	119.24, CH_{Ar}	C2, C4a
5	7.66, d (8.0)	118.58, CH_{Ar}	C10a, C7, C8a	7.61, d (8.6)	118.48, CH_{Ar}	C7, C8a, C10a
6	7.91, t	137.10, CH_{Ar}	C10a	7.87, t	136.12, CH_{Ar}	C10a
7	7.50, t	125.44, CH_{Ar}	C5	7.42, t	125.18, CH_{Ar}	C5, C8a
8	8.17, d (8.0)	126.04, CH_{Ar}	C6, C9, C10a	8.05, d (8.1)	126.45, CH_{Ar}	C6, C9, C10a
4a	-	157.71, C	-	-	149.97, C	-
8a	-	120.44, C	-	-	122.02, C	-
9a	-	107.06, C	-	-	115.06, C	-
10a	-	156.20, C	-	-	155.35, C	-
9	-	181.67, C=O	-	-	175.26, C=O	-
1’	-	164.58, C=O	-	-	165.38, C=O	-
2’	6.90, d (16.0)	117.17, C=C	C4’, C1’	6.97, d (16.0)	118.05, C=C	C1’, C4’
3’	7.89, d (16.0)	147.94, C=C	C1’, C2’, C5’	7.86, d (16.0)	146.83, C=C	C1’, C2’, C5’
4’	-	134.28, C	-	-	134.47, C	-
5’	7.81, m	129.61, CH_{Ar}	C6’	7.86, m	129.60, CH_{Ar}	C7’
6’	7.44, m	129.37, CH_{Ar}	C4’	7.43, m	129.22, CH_{Ar}	C4’
7’	7.45, m	131.70, CH_{Ar}	C6’, C6”	7.43, m	131.43, CH_{Ar}	C5’
5”	7.81, m	129.61, CH_{Ar}	C6”	7.86, m	129.60, CH_{Ar}	C7’
6”	7.44, m	129.37, CH_{Ar}	C4’	7.43, m	129.22, CH_{Ar}	C4’
OH	12.78, s	-	C3, C4	-	-	-

The ^{1}H-NMR of compounds **4a**-**d** showed two characteristic signals of proton bound to the α,β-unsaturated ester of hybrid xanthyl-cinnamate structure at δ_H 6.87–6.97 and 7.86–7.90 ppm corresponding to the H2' and H3', respectively. Large *J* values (16.0 Hz) at H2' and H3' indicated the presence of trans-double bonds. Meanwhile, their ^{13}C-NMR spectra showed C–O signals at 156.20–158.35 ppm corresponding to the ester group of xanthyl-cinnamate and two carbonyl signals at δ_C 175.26–181.67 and 164.58–166.55 ppm corresponding to the carbonyl group of xanthone and cinnamate, respectively (Tables 1 and 2). It was found that the reaction between compound **3c** and cinnamoyl chloride produced two isomeric products, **4c** and **4d**. The ^{1}H- and ^{13}C-NMR spectra proved this reaction produced two products, and LC-MS detected the same molecular mass at *m/z* equal to 375. This phenomenon occurred due to the gradual addition of 2 equivalents of cinnamoyl chloride as an acylation reagent to the reaction. Compound **3c** has three OH substituents, making a high probability of obtaining a xanthyl-cinnamate isomer using K_2CO_3 via esterification. This phenomenon was not observed in the synthesis reaction of **4a** and **4b**.

In Vitro Cytotoxicity Evaluation

The cytotoxic effect of xanthyl-cinnamate was evaluated using the MTT test on four human cancer cell lines, i.e., HeLa, T47D, A549, and WiDr (Table 3). All xanthyl-cinnamate compounds exhibited no anticancer activity against HeLa, while only compound **4d** exhibited a weak inhibitory impact against A549 [21]. Out of the seven compounds tested, compounds **4c** and **4d** gave lower IC_{50} values than compounds **4a** and **4b**, meaning that these compounds have higher anticancer activity.

Table 2. ^{1}H- and ^{13}C-NMR spectra data for compounds 1,3-dihydroxyxanthen-6-yl cinnamate (**4c**) and 3,6-dihydroxyxanthen-1-yl cinnamate (**4d**)

Position	**4c**		**4d**	
	δ_H (*J* in Hz)	δ_C, type	δ_H (*J* in Hz)	δ_C, type
1	-	163.43, C–OH	-	158.35, CO
2	6.20, d (2.1)	98.90, CH_{Ar}	6.84, d (2.2)	102.64, CH_{Ar}
3	-	164.80, C–OH	-	164.63, C–OH
4	6.37, d (2.1)	94.76, CH_{Ar}	6.68, d (2.0)	101.73, CH_{Ar}
5	7.53, d (2.2)	111.53, CH_{Ar}	6.95, d (2.1)	105.03, CH_{Ar}
6	-	158.08, CO	-	162.57, C–OH
7	7.32, dd (8.7, 2.2)	118.28, CH_{Ar}	6.93, dd (8.8, 2.1)	112.86, CH_{Ar}
8	8.15, d (8.7)	127.30, CH_{Ar}	8.01, d (8.8)	131.67, CH_{Ar}
4a	-	156.60, C	-	157.05, C
8a	-	102.63, C	-	115.30, C
9a	-	119.49, C	-	106.50, C
10a	-	156.21, C	-	156.82, C
9	-	179.67, C=O	-	180.50, C=O
1'	-	166.55, C=O	-	165.67, C=O
2'	6.91, d (16.0)	117.13, C=C	6.87, d (16.0)	117.20, C=C
3'	7.90, d (16.0)	147.95, C=C	7.88, d (16.0)	147.85, C=C
4'	-	134.26, C	-	134.28, C
5'	7.80, m	129.60, CH_{Ar}	7.79, m	129.35, CH_{Ar}
6'	7.44, m	129.37, CH_{Ar}	7.44, m	131.67, CH_{Ar}
7'	7.44, m	131.70, CH_{Ar}	7.44, m	128.09, CH_{Ar}
5"	7.80, m	129.60, CH_{Ar}	7.79, m	129.35, CH_{Ar}
6"	7.44, m	129.37, CH_{Ar}	7.44, m	131.67, CH_{Ar}
OH	12.73, s	-	13.04, s	-

Table 3. The *in vitro* MTT assay of the tested compounds against human cancer cell lines and Vero normal cell line

Compound	IC_{50} (μM)[a]				
	T47D	HeLa	A549	WiDr	Vero
3a	137.24	85.75	124.96	114.47	307.94
3b	248.82*	1197.55	> 471.70[b]	1111.23*	7562.64
3c	121.89	203.16	163.61	141.19	456.89
4a	298.94	2398.69	371.15	122.43*	5739.72
4b	549.33	2958.83*	247.66*	104.47*	8330.91
4c	110.29	202.86	458.29	39.57	1051.76
4d	62.46	204.36	61.90	57.62	827.14
Doxorubicin	32.80	-	-	3.73	3171.77
Cisplatin	-	68.42	82.00	-	168.68

[a]All values are expressed as the mean of once or twice biological replicates determinations. [b]Value has given because the compound could not reach a 50% inhibition at the highest compound concentration. *The experiments were done only in technical triplicates

Table 4. Selectivity index of tested compounds as an anticancer agent

Compound	Selectivity Index (SI)[a,b]			
	T47D	HeLa	A549	WiDr
3a	2.30	4.52	2.47	4.50
3b	30.40*	6.67	>16.03	6.81*
3c	3.79	2.55	3.18	20.18
4a	48.67	8.14	209.03	43.83*
4b	23.10	2.82*	33.64*	79.73*
4c	9.62	6.45	2.75	31.44
4d	14.37	4.37	13.71	24.74
Doxorubicin	220.08	-	-	866.65
Cisplatin	-	2.62	2.31	-

[a]All values are expressed as the mean of once or twice biological replicates determinations. [b]SI value = IC_{50} value of Vero/IC_{50} value of cancer cell. *The experiments were done only in technical triplicates

Compounds **4c** and **4d** possessing two hydroxy groups bound to the xanthone ring displayed the dominant cytotoxic activity compared to other xanthyl-cinnamate compounds, which resulted in lower IC_{50} values. In particular, compound **4c** with an IC_{50} value of 39.57 μM exhibited a moderate cytotoxic effect against WiDr, according to [21]. The results showed that the presence of the hydroxy group in the xanthone ring improved the cytotoxicity of the compound. The differences in cinnamate position in the xanthone ring (**4c** and **4d**) nearly have no significant effect on the compound activity.

Selectivity index (SI) determination is a vital indicator of a compound's cytotoxicity evaluation, which indicates selective cytotoxicity of the compounds in the malignant cells to the normal cells. Cytotoxicity assay on Vero cells was selected as a standard for determining the selectivity of the compounds. The cinnamate moiety in the xanthone displayed a selective effect with higher IC_{50} values (827.14–8330.91 μM) to Vero cells than the corresponding oxygenated-xanthone (307.94–7562.64 μM). As shown in Table 4, SI values of **4a**-**d** compounds (2.75–209.03) passed the parameter SI higher than two according to [22], while oxygenated-xanthone (**3a**-**c**) showed lower SI values (2.30–30.40). This result demonstrates that cinnamate moiety addition increased the selectivity properties of xanthones as anticancer agents, which is remarkable as selectivity is a desirable property in a drug [23].

Although no dramatic changes were observed from the xanthone modification, the cytotoxic activity of

xanthyl-cinnamates against four cancer cell lines gave IC_{50} values similar to the parent compounds (Table 3), especially on compounds **4c** and **4d**, which have the best cytotoxic activity between the hybrid molecules. Animal testing *in vivo* assays should be carried on the research to optimize the *in vitro* cytotoxic assay results. Using simplified *in vitro* assays may not be optimum, as there is a paradigm that refers to an uncritical hunt for "nanomolar potent" drugs using *in vitro* assays, which can create false positives in selecting a drug candidate [24].

Molecular Docking Studies

The molecular docking studies of the synthesized compounds into the EGFR binding pocket were performed to explain the possible binding modes of these xanthone derivatives with EGFR. The over-expression activity of EGFR was reported in T47D, HeLa, A549, and WiDr cell lines [25-28]. The method used in this study has been through validation with redocking to set the grid box.

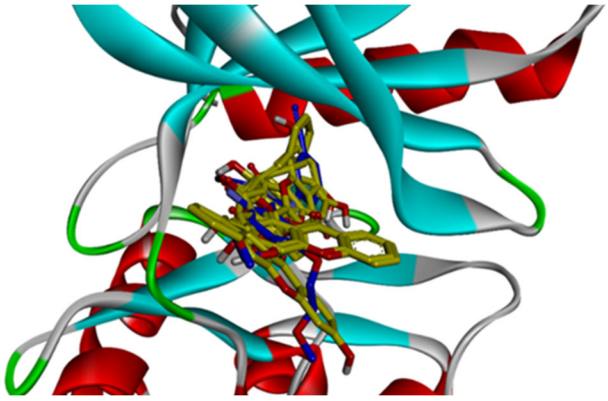

Fig 2. Overlay of 7 synthesized compounds (yellow) and erlotinib (navy) positions in the EGFR binding site

Table 5. Molecular docking results of the synthesized compounds

Compound	ΔG (kJ/mol)	Ki (μM)	Hydrogen Bond
3a	-25.65	32.23	MET769, GLN767, THR766
3b	-25.19	38.46	MET769, GLN767, THR766
3c	-28.28	11.12	MET769, GLN767, THR766, LYS721
4a	-35.48	0.61	MET769
4b	-34.10	1.06	MET769
4c	-33.77	1.22	MET769, THR766, LYS721, ASP831
4d	-35.02	0.74	MET769, ASP776, PRO770
erlotinib	-29.62	6.46	MET769, CYS773

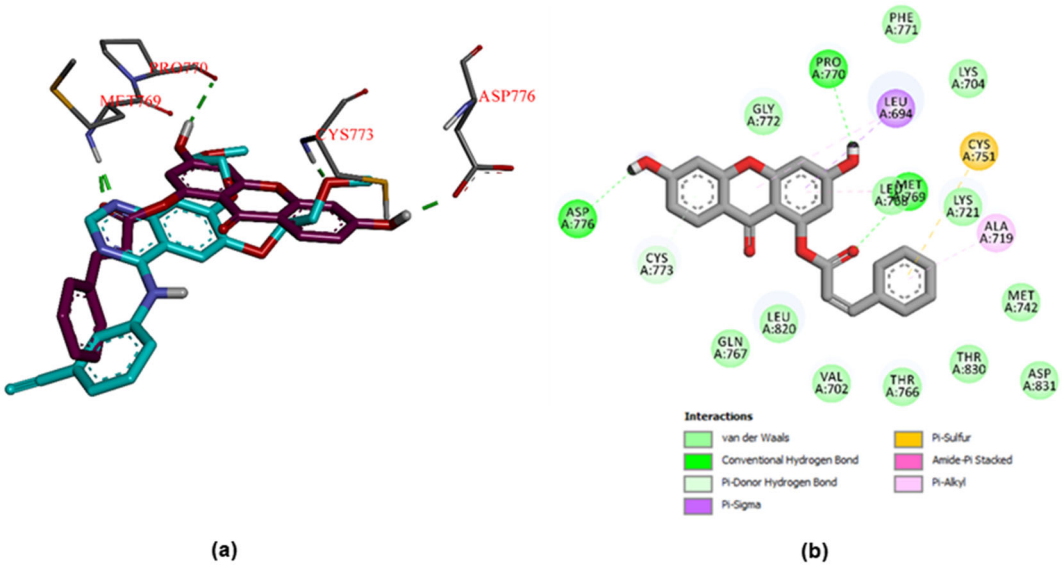

Fig 3. (a) The 3D structure of **4d** (magenta) binding mode in EGFR overlay with erlotinib (blue) position in the active site of EGFR protein; hydrogen bonding interaction shows in green lines, and (b) the 2D structure of **4d** interaction with amino acid residues of the EGFR protein

Redocking of erlotinib in EGFR gives an RMSD value of 1.56 Å and ΔG value of -29.62 kJ/mol. Erlotinib, an EGFR-competitive inhibitor, interacted in the same spot of the ATP-EGFR complex. Erlotinib-EGFR interaction stabilized by two hydrogen bonds of N atom with MET769 and O atom with CYS773 [29].

All synthesized compounds that docked into the EGFR gave a similar spot to that of erlotinib, with MET769 as the benchmark (Fig. 2). The details molecular docking results (3D and 2D structures) of all synthesized compounds are presented in the Supplementary Data. The docking analysis of the four xanthyl-cinnamate compounds suggested that these compounds may interact with the EGFR active site more effectively than their parent compounds (Table 5). The complex of **4d**-EGFR was chosen as the best binding mode with a ΔG value of -35.02 kJ/mol and a Ki value of 0.74 μM. In the binding model, compound **4d** with three oxygen atoms from the carboxyl and hydroxy groups establishes hydrogen bonds with MET769, ASP776, and PRO770 without detectable unfavorable donor-donor interactions in the complex (Fig. 3(a) and (b)).

■ CONCLUSION

A novel series of xanthyl-cinnamate was synthesized and evaluated as an anticancer agent. The present study shows that xanthyl-cinnamate compounds represent a promising cytotoxic activity, especially for compounds **4c** and **4d**. Molecular hybridization of xanthone and cinnamic acid (**4a**-**d**) resulted in a higher selectivity (SI = 2.75–209.03) compared to oxygenated-xanthone (**3a**-**c**) (SI = 2.30–30.40). Furthermore, compound **4c** was chosen as a promising drug candidate for colon cancer as it exhibited moderate cytotoxic activity with an IC_{50} value of 39.57 μM against WiDr cell lines. The molecular docking studies of the synthesized compounds showed that all xanthyl-cinnamate (**4a**-**d**) exhibited a greater binding affinity than its parental molecules (**3a**-**c**) and erlotinib in the EGFR binding site.

■ ACKNOWLEDGMENTS

The authors would like to express gratitude to KEMENDIKBUD-RISTEK for the financial support for this research and the *Pendidikan Magister Menuju Doktor Untuk Sarjana Unggul* (PMDSU) scholarship for Muthia Rahayu Iresha. We would also like to thank Austrian-Indonesian Centre (AIC) for Computational Chemistry for the Gaussian 09 license that has been provided.

■ REFERENCES

[1] Sung, H., Ferlay, J., Siegel, R.L., Laversanne, M., Soerjomataram, I., Jemal, A., and Bray, F., 2021, Global cancer statistics 2020: GLOBOCAN estimates of incidence and mortality worldwide for 36 cancers in 185 countries, *CA Cancer J. Clin.*, 71 (3), 209–249.

[2] Schirrmacher, V., 2019, From chemotherapy to biological therapy: A review of novel concepts to reduce the side effects of systemic cancer treatment, *Int. J. Oncol.*, 54 (2), 407–419.

[3] Zhang, C., Yu, G., and Shen, Y., 2018, The naturally occurring xanthone α-mangostin induces ROS-mediated cytotoxicity in non-small scale lung cancer cells, *Saudi J. Biol. Sci.*, 25 (6), 1090–1095.

[4] Kaewpiboon, C., Boonnak, N., Yawut, N., Kaowinn, S., and Chung, Y.H., 2019, Caged-xanthone from *Cratoxylum formosum* ssp. *pruniflorum* inhibits malignant cancer phenotypes in multidrug-resistant human A549 lung cancer cells through down-regulation of NF-κB, *Bioorg. Med. Chem.*, 27 (12), 2368–2375.

[5] Wu, J., Dai, J., Zhang, Y., Wang, J., Huang, L., Ding, H., Li, T., Zhang, Y., Mao, J., and Yu, S., 2019, Synthesis of novel xanthone analogues and their growth inhibitory activity against human lung cancer A549 cells, *Drug Des., Dev. Ther.*, 13, 4239–4246.

[6] Pinto, M.M.M., Palmeira, A., Fernandes, C., Resende, D.I.S.P., Sousa, E., Cidade, H., Tiritan, M.E., Correia-da-Silva, M., and Cravo, S., 2021, From natural products to new synthetic small molecules: A journey through the world of xanthones, *Molecules*, 26 (2), 431.

[7] Fatmasari, N., Kurniawan, Y.S., Jumina, J., Anwar, C., Priastomo, Y., Pranowo, H.D., Zulkarnain, A.K., and Sholikhah, E.N., 2022, Synthesis and *in vitro*

assay of hydroxyxanthones as antioxidant and anticancer agents, *Sci. Rep.*, 12 (1), 1535.

[8] Yuanita, E., Pranowo, H.D., Mustofa, M., Swasono, R.T., Syahri, J., and Jumina, J., 2019, Synthesis, characterization and molecular docking of chloro-substituted hydroxyxanthone derivatives, *Chem. J. Mold.*, 14 (1), 68–76.

[9] Takahashi, T., and Miyazawa, M., 2010, Tyrosinase inhibitory activities of cinnamic acid analogues, *Pharmazie*, 65, 913–918.

[10] de Oliveira Niero, E.L., and Machado-Santelli, G.M., 2013, Cinnamic acid induces apoptotic cell death and cytoskeleton disruption in human melanoma cells, *J. Exp. Clin. Cancer Res.*, 32 (1), 31.

[11] Keawsa-ard, S., Natakankitkul, S., Liawruangrath, S., Teerawutkulrag, A., Trisuwan, K., Charoenying, P., Pyne, S.G., and Liawruangrath, B., 2012, Anticancer and antibacterial activities of the isolated compounds from *Solanum spirale* Roxb. leaves, *Chiang Mai J. Sci.*, 39 (3), 445–454.

[12] do Vale, J.A., Rodrigues, M.P., Lima, A.M.A., Santiago, S.S., Lima, G.D.A., Almeida, A.A., de Oliveira, L.L., Bressan, G.C., Teixeira, R.R., and Machado-Neves, M., 2022, Synthesis of cinnamic acid ester derivatives with antiproliferative and antimetastatic activities on murine melanoma cells, *Biomed. Pharmacother.*, 148, 112689.

[13] Ruwizhi, N., and Aderibigbe, B.A., 2020, Cinnamic acid derivatives and their biological efficacy, *Int. J. Mol. Sci.*, 21 (16), 5712.

[14] Ge, Y.X., Wang, Y.H., Zhang, J., Yu, Z.P., Mu, X., Song, J.L., Wang, Y.Y., Yang, F., Meng, N., Jiang, C.S., and Zhang, H., 2019, New cinnamic acid-pregenolone hybrids as potential antiproliferative agents: Design, synthesis and biological evaluation, *Steroids*, 152, 108499.

[15] Ruan, B.F., Ge, W.W., Cheng, H.J., Xu, H.J., Li, Q.S., and Liu, X.H., 2017, Resveratrol-based cinnamic ester hybrids: Synthesis, characterization, and anti-inflammatory activity, *J. Enzyme Inhib. Med. Chem.*, 32 (1), 1282–1290.

[16] Deng, Z., Li, C., Luo, D., Teng, P., Guo, Z., Tu, X., Zou, K., and Gong, D., 2017, A new cinnamic acid derivative from plant-derived endophytic fungus *Pyronema* sp., *Nat. Prod. Res.*, 31 (20), 2413–2419.

[17] Xu, C.C., Deng, T., Fan, M.L., Lv, W.B., Liu, J.H., and Yu, B.Y., 2016, Synthesis and *in vitro* antitumor evaluation of dihydroartemisinin-cinnamic acid ester derivatives, *Eur. J. Med. Chem.*, 107, 192–203.

[18] Shang, H., Li, L., Ma, L., Tian, Y., Jia, H., Zhang, T., Yu, M., and Zou, Z., 2020, Design and synthesis of molecular hybrids of sophora alkaloids and cinnamic acids as potential antitumor agents, *Molecules*, 25 (5), 1168.

[19] Das, A., Shaikh, M.M., and Jana, S., 2014, Design, synthesis, and *in vitro* antibacterial screening of some novel 3-pentyloxy-1-hydroxyxanthone derivatives, *Med. Chem. Res.*, 23 (1), 436–444.

[20] Iresha, M.R., Jumina, J., and Pranowo, H.D., 2020, Molecular docking study of xanthyl chalcone derivatives as potential inhibitor agents against KIT tyrosine kinase and KIT kinase domain mutant D816H, *J. Appl. Pharm. Sci.*, 10 (11), 18–26.

[21] Miladiyah, I., Jumina, J., Haryana, S.M., and Mustofa, M., 2018, Biological activity, quantitative structure-activity relationship analysis, and molecular docking of xanthone derivatives as anticancer drugs, *Drug Des., Dev. Ther.*, 12, 149–158.

[22] Badisa, R.B., Darling-Reed, S.F., Joseph, P., Cooperwood, J.S., Latinwo, L.M., and Goodman, C.B., 2009, Selective cytotoxic activities of two novel synthetic drugs on human breast carcinoma MCF-7 cells, *Anticancer Res.*, 29 (8), 2993–2996.

[23] Mencher, S.K., and Wang, L.G., 2005, Promiscuous drugs compared to selective drugs (promiscuity can be a virtue), *BMC Clin. Pharmacol.*, 5 (1), 3.

[24] Wong, C.C., Cheng, K.W., and Rigas, B., 2012, Preclinical predictors of anticancer drug efficacy: Critical assessment with emphasis on whether nanomolar potency should be required of candidate agents, *J. Pharmacol. Exp. Ther.*, 341 (3), 572–578.

[25] Jung, K.H., Lee, E.J., Park, J.W., Lee, J.H., Moon, S.H., Cho, Y.S., and Lee, K.H., 2019, EGF receptor stimulation shifts breast cancer cell glucose metabolism toward glycolytic flux through PI3 kinase signaling, *PLoS One*, 14 (9), e0221294.

[26] McGaffin, K.R., Acktinson, L.E., and Chrysogelos, S.A., 2004, Growth and EGFR regulation in breast cancer cells by vitamin D and retinoid compounds, *Breast Cancer Res. Treat*., 86 (1), 55–73.

[27] Qian, Y., Qiu, M., Wu, Q., Tian, Y., Zhang, Y., Gu, N., Li, S., Xu, L., and Yin, R., 2014, Enhanced cytotoxic activity of cetuximab in EGFR-positive lung cancer by conjugating with gold nanoparticles, *Sci. Rep*., 4 (1), 7490.

[28] Shigeta, K., Hayashida, T., Hoshino, Y., Okabayashi, K., Endo, T., Ishii, Y., Hasegawa, H., and Kitagawa, Y., 2013, Expression of epidermal growth factor receptor detected by cetuximab indicates its efficacy to inhibit *in vitro* and *in vivo* proliferation of colorectal cancer cells, *PLoS One*, 8 (6), e66302.

[29] Stamos, J., Sliwkowski, M.X., and Eigenbrot, C., 2002, Structure of the epidermal growth factor receptor kinase domain alone and in complex with a 4-anilinoquinazoline inhibitor, *J. Biol. Chem.*, 277 (48), 46265–46272.